HE 2.1.2

HADRON DISTRIBUTIONS IN THE CORE OF 100 TeV EXTENSIVE AIR SHOWERS

J. Unger* for the KASCADE Collaboration†

Forschungszentrum Karlsruhe, Institut für Kernphysik, D-76021 Karlsruhe, Germany

ABSTRACT

With the central hadron calorimeter of the KASCADE experiment the cores of extensive air showers corresponding to primary energies around 100 TeV are investigated. The accurate position of the shower core is determined with a scintillator array on top of the calorimeter or with the upper layer of ionisation chambers in the calorimeter. The rates, energy spectrum and lateral distributions of hadrons are obtained and compared with simulations using the CORSIKA code. The interaction models VENUS and QGSJET turned out to describe the data reasonably well. Differences between data and models are discussed.

INTRODUCTION

The experiment KASCADE (Klages et al., 1997) has in its center a large iron calorimeter to study the hadronic core of large extensive air showers (EAS) in the energy region around the "knee". The hadronic component is important when investigating the high energy nuclear interaction on one hand and the mass composition of primary cosmic rays on the other hand. In order to distinguish the effects of primary composition from those of collision characteristics it has become apparent that all components of an EAS have to be measured simultaneously and their correlations to be studied. Among the components which are particularly sensitive to changes in collision characteristics and primary composition are the high energy hadrons which constitute the backbone and skeleton of air showers and are concentrated close to the core.

THE APPARATUS

Hadron detectors are necessarily complicated devices since they have not only to detect individual hadrons and to disentangle them from each other, but also have to measure their energy separately. The KASCADE calorimeter uses iron as absorber and liquid ionisation chambers interspersed between the slabs as active devices. As liquid tetramethylsilane and tetramethylpentane are used. Ionisation chambers offer several advantages especially for usage in a cosmic ray experiment (Engler, 1996). Their signals are directly proportional to the deposited energy and do not saturate, offering a large dynamic range. Feed-back controlled amplification ensures stable operation over long periods of time, particularly important for a ten year experiment located on the lawn without any temperature stabilization. With the high density of a liquid, an absolute energy calibration is feasible by using the energy deposition of through–going muons.

The heart of the central detector is a massive absorber block of cast ion slabs. On top of the iron a 5 cm lead filter ensures an efficient absorption of the electromagnetic component shielding the first layer of ionisation chambers by 15 radiation lengths. The depth of the calorimeter corresponds to 11 nuclear interaction lengths, and the amplifier chain allows to measure energy depositions up to 9 GeV per channel, corresponding to 10^4 traversing muons. Hence, hadrons are detected up to 10 TeV without being restrained by leakage or saturation effects as discussed by Milke (Milke et al., 1997). The ionisation chambers have finely segmented

*corresponding author, email: joerg@ik1.fzk.de

†A full list of authors and institutions of the KASCADE Collaboration is given at the end of this volume.

electrodes of $25 \times 25 \mathrm{cm}^2$ size matched to the mean lateral spread of hadronic cascades, allowing to resolve single hadrons in the core of large EAS.

The hadron recognition proceeds as follows: firstly, local maxima of energy are looked for in each layer of chambers. Secondly, the direction of the infalling hadrons is found approximately by using the upper four layers. The alignment of maxima is then tested starting from the lowest layer as the most quiet environment and checked for coincidence with the approximate directions. For a hadron track to be accepted at least three local maxima have to contribute. Finally, the energy in surrounding channels is allocated to the track. Depending on the activity in the neighbouring channels, energy is collected within a radius of up to four electrode pads. The efficiency for reconstruction of protons at two different zenith angles is plotted in Figure 1. About 50% efficiency for 50 GeV protons and full efficiency around 100 GeV is achieved. The algorithm ensures muon rejection below the 1% level up to 1 TeV, where muons in iron start to radiate. How well individual hadrons can be resolved laterally is demonstrated in Figure 2. Shown is the probability that two parallel incident protons are recognized as separate particles. It can be seen that in the mean two hadrons are separated if they are 50 cm apart.

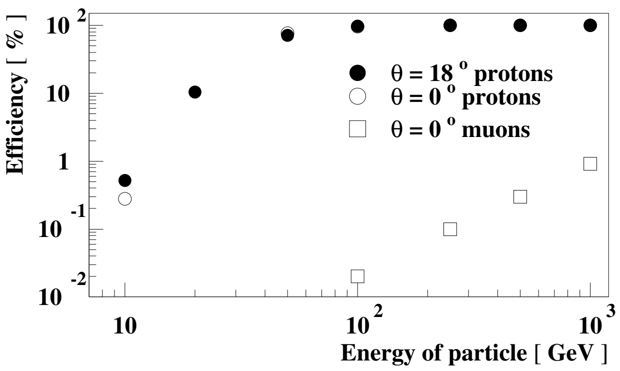

Fig. 1: Efficiency for hadron reconstruction vs. hadron energy for different zenith angels Θ.

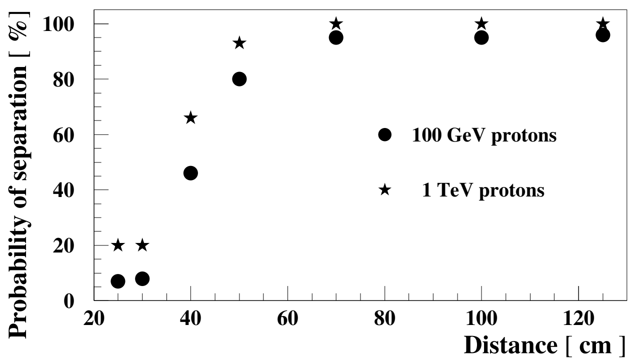

Fig. 2: Probability of separation vs. distance between hadrons.

RESULTS

The present analysis concentrates on low energy showers near the KASCADE threshold, where the primary mass spectrum is reasonably well known. The primary flux values are taken from a compilation by B. Wiebel (Wiebel, 1994). In this energy region below 1 PeV the data allow to distinguish between different interaction models, as implemented in CORSIKA (Heck et al., 1997). The trigger requires an 8 fold coincidence of scintillators in the trigger layer, i.e. in most cases caused by muons.

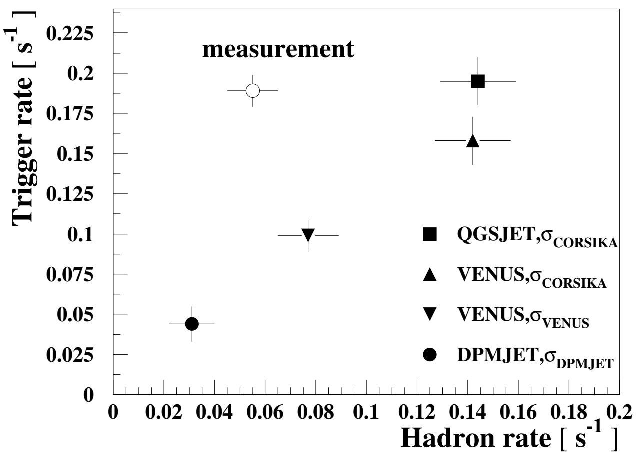

Fig. 3: Trigger rate vs. rate of events with at least one reconstructed hadron.

The trigger rates per se are very sensitive to the interaction models, in particular to the inelastic cross-sections used to transport the particles between collisions. This is demonstrated in Figure 3 which shows the trigger rate versus the hadron rate, that is the rate of events in which at least one hadron with an energy greater than 50 GeV has been reconstructed. One observes that both models VENUS and QGSJET reproduce the trigger rates reasonably well but predict too many hadrons. This might indicate that the inelastic cross-sections used in CORSIKA might be too low causing a late shower development, and a high hadron content as a consequence.

Therefore, larger cross-sections have been tried, e.g. those given by the VENUS model, which are higher than the original CORSIKA values. As expected, fewer hadrons reach the observation level. But also reduced is the trigger rate, which should be less effected because, due to muons, the trigger should be of more integral character. A trigger composed of penetrating muons should be not very sensitive to the height of shower development, whereas hadrons are. The matter needs further investigation.

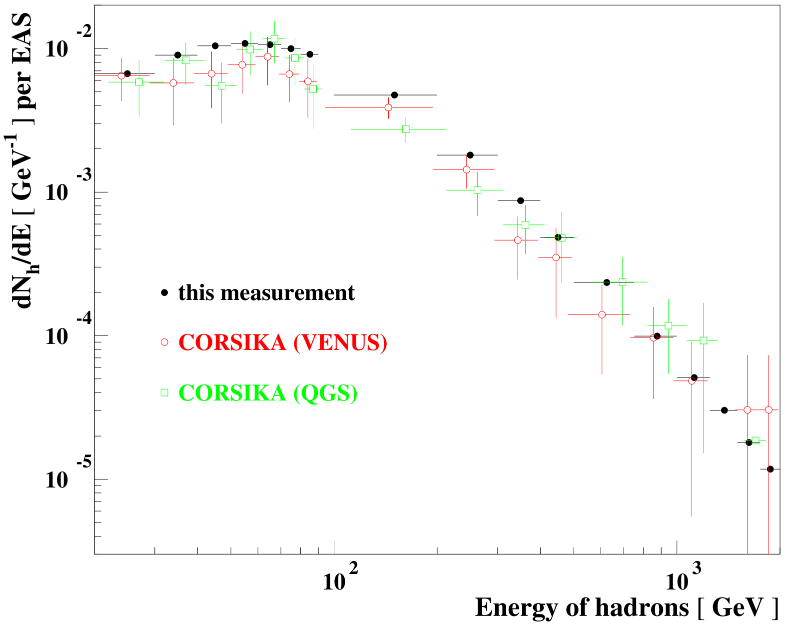

Fig. 4: Energy distribution of hadrons in showers with $N_e \approx 10^5$ *mean electron size.*

The energy distribution of hadrons in the cores of EAS is given in Figure 4. Plotted is the frequency of reconstructed hadrons with respect to their energy compared with simulated events using the VENUS and QGSJET code. The flattening in the power law spectrum below 100 GeV is caused by the decreasing detection efficiencies at low energies.

Apart from the total rate problem one observes that also in the energy distribution slight differences exist between measurements and simulations. The VENUS model seems to fit the data best.

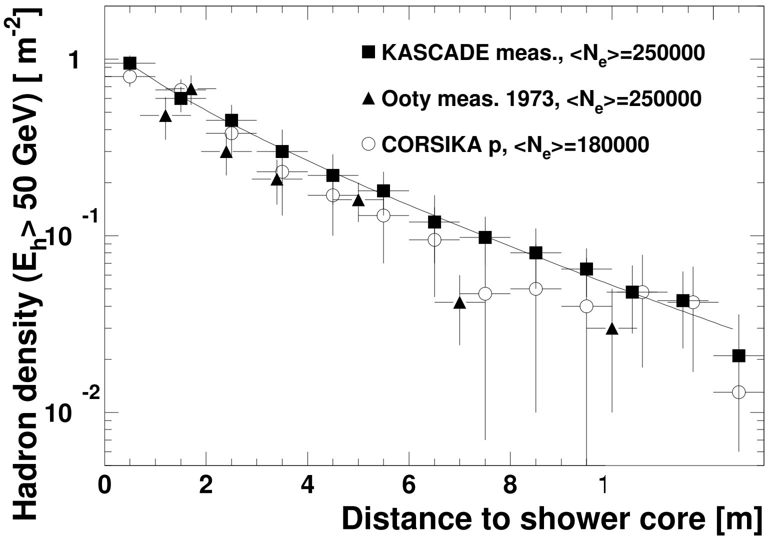

Fig. 5: Lateral hadron distribution for all hadrons.

How the present investigations compare with measurements as published in literature is demonstrated in Figures 5 and 6. Shown are lateral hadron distributions with respect to the shower center for all hadrons and for high energy hadrons only. For this comparison the shower center has to be known as exactly as possible. Therefore, only such events were selected in which enough electromagnetic energy was found in the first layer of ionisation chambers. The data are classified according to the electron shower size N_e. In this way measurements performed on different observation levels should be comparable because in an EAS on its way through the atmosphere the number of electrons is approximately proportional to the number of 100 GeV hadrons (Kempa, 1976).

In Figure 5 it can be seen that the present measurements compare well with hadron distributions obtained at Ooty located at mountain level corresponding to 800 g cm^{-2} for showers with $N_e = 250000$ (Vatcha and Sreekantan, 1973). The lines shown are heuristic fits to the data using the ansatz $\rho = Ae^{-(r/r_0)^n}$ with $n \approx 0.8$. Also, the distribution for high energy hadrons agrees reasonably well with data measured by the Tien-Shan group at a level of 690 g cm^{-2} (Danilova et al., 1985) as is demonstrated in Figure 6.

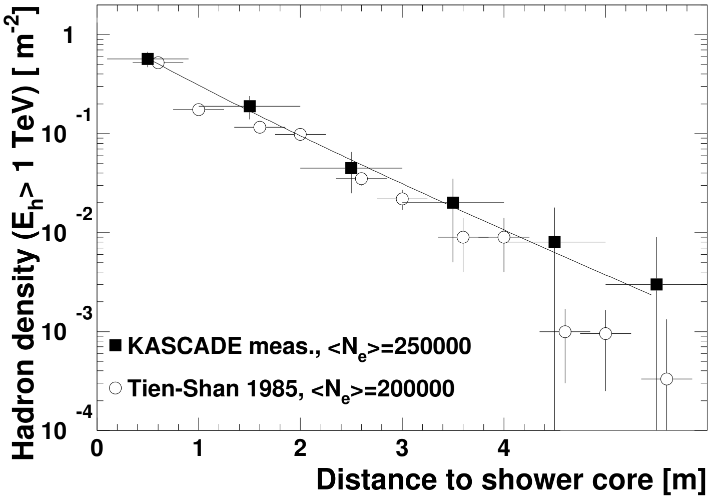

Fig. 6: Lateral distribution for high energy hadrons.

CONCLUSION

The first data obtained with the KASCADE calorimeter exhibit reliable performance and compare well with previous measurements. Analysis of EAS cores with primary energies in the 100 TeV region, where the primary composition is reasonably well known, allows a detailed test of interaction models and simulation codes.

ACKNOWLEDGMENT

This work was partly supported by the Polish State Committee for Scientific Research (grant Nr. 2P03B 160 12).

REFERENCES

Danilova, T.V. et al., *Proc. 19th ICRC, La Jolla* **7**, 40 (1985).
Engler, J., *J. Phys. G: Nucl. Part. Phys.* **22**, 1 (1996).
Heck, D., Knapp, J. et al., *Proc.* 25^{th} *ICRC*, Durban, **HE 2.3.2** (1997).
Kempa, J., *Nuovo Cimento* **31A**, 568(1976).
Klages, H.O. et al., *Nucl. Phys. B (Proc. Suppl.)*, **52B**, 92, (1997).
Milke, J. et al., *Proc.* 25^{th} *ICRC*, **HE 1.2.28** (1997).
Vatcha, R.H. and Sreekantan, B.V., *J.Phys.A: Math., Nucl.Gen.* **6**, 1050 (1973).
Wiebel, B., Chemical composition in high energy cosmic rays, Bergische Universität Wuppertal **WUB 94-08**.